Title

Muscle mitochondrial stress adaptation operates independently of endogenous FGF21 action

Journal

Molecular Metabolism, 5(2)

ISSN

2212-8778

Authors

Ost, Mario
Coleman, Verena
Voigt, Anja
et al.

Publication Date

2016-02-01

DOI

10.1016/j.molmet.2015.11.002

Peer reviewed

Original article

MOLECULAR METABOLISM

Muscle mitochondrial stress adaptation operates independently of endogenous FGF21 action

Mario Ost [1,*,6], Verena Coleman [1,6], Anja Voigt [1], Evert M. van Schothorst [2], Susanne Keipert [3], Inge van der Stelt [2], Sebastian Ringel [1], Antonia Graja [4], Thomas Ambrosi [4], Anna P. Kipp [5], Martin Jastroch [3], Tim J. Schulz [4], Jaap Keijer [2], Susanne Klaus [1]

ABSTRACT

Objective: Fibroblast growth factor 21 (FGF21) was recently discovered as stress-induced myokine during mitochondrial disease and proposed as key metabolic mediator of the integrated stress response (ISR) presumably causing systemic metabolic improvements. Curiously, the precise cell-non-autonomous and cell-autonomous relevance of endogenous FGF21 action remained poorly understood.

Methods: We made use of the established UCP1 transgenic (TG) mouse, a model of metabolic perturbations made by a specific decrease in muscle mitochondrial efficiency through increased respiratory uncoupling and robust metabolic adaptation and muscle ISR-driven FGF21 induction. In a cross of TG with *Fgf21*-knockout (FGF21$^{-/-}$) mice, we determined the functional role of FGF21 as a muscle stress-induced myokine under low and high fat feeding conditions.

Results: Here we uncovered that FGF21 signaling is dispensable for metabolic improvements evoked by compromised mitochondrial function in skeletal muscle. Strikingly, genetic ablation of FGF21 fully counteracted the cell-non-autonomous metabolic remodeling and browning of subcutaneous white adipose tissue (WAT), together with the reduction of circulating triglycerides and cholesterol. Brown adipose tissue activity was similar in all groups. Remarkably, we found that FGF21 played a negligible role in muscle mitochondrial stress-related improved obesity resistance, glycemic control and hepatic lipid homeostasis. Furthermore, the protective cell-autonomous muscle mitohormesis and metabolic stress adaptation, including an increased muscle proteostasis via mitochondrial unfolded protein response (UPR^{mt}) and amino acid biosynthetic pathways did not require the presence of FGF21.

Conclusions: Here we demonstrate that although FGF21 drives WAT remodeling, the adaptive pseudo-starvation response under elevated muscle mitochondrial stress conditions operates independently of both WAT browning and FGF21 action. Thus, our findings challenge FGF21 as key metabolic mediator of the mitochondrial stress adaptation and powerful therapeutic target during muscle mitochondrial disease.

Keywords Browning; FGF21; GDF15; Myokine; Mitochondrial disease; Muscle mitohormesis

1. INTRODUCTION

During the last decade, the pleotropic hormone-like circulating protein fibroblast growth factor 21 (FGF21) gained momentum as a major metabolic regulator in metabolism and disease [1–4]. Notably, FGF21 was found to be expressed not only in liver [5] and white adipose tissue (WAT) [6] but also in skeletal muscle [7]. A first study linking muscle FGF21 secretion to mitochondrial dysfunction and pseudo-starvation described the Deletor mouse, a model of late-onset mitochondrial myopathy [8]. Subsequently, significant elevations of circulating FGF21 levels were demonstrated in muscle-specific mouse models of autophagy deficiency [9] and have been associated with a mild decrease in mitochondrial efficiency [10] as well as activation of mTOR complex1 (mTORC1) signaling [11]. In humans, muscle FGF21 expression is induced by hyperinsulinemia [12] but not by exercise [13]. In patients, the constitutive secretion of FGF21 is accepted as the common denominator of muscle stress conditions and mitochondrial disease [14,15]. Based on these important clinical findings, a role of endogenous FGF21 for systemic energy metabolism has been proposed [16]. So far, the major targets and metabolic functions of stress-induced muscle FGF21 are poorly understood and await experimental establishment of causality.

Liver and adipose tissue are considered as the main targets of the myokine FGF21, but not skeletal muscle, due to lack of the FGF-receptor cofactor β-klotho [10,17]. However, an endocrine axis of FGF21 is established as it regulates adiponectin in adipocytes, thus coupling FGF21 action in WAT to metabolic effects in liver and muscle [18]. This strongly supports bidirectional muscle-WAT crosstalk. Moreover, as an adipokine, FGF21 promotes brown adipose tissue (BAT)-like structures within WAT depots in response to cold exposure

[1]Research Group Physiology of Energy Metabolism, German Institute of Human Nutrition, Nuthetal, 14558, Germany [2]Human and Animal Physiology, Wageningen University, Wageningen, 6708, Netherlands [3]Helmholtz Diabetes Center, Helmholtz Zentrum München, Neuherberg, 85764, Germany [4]Research Group Adipocyte Development, German Institute of Human Nutrition, Nuthetal, 14558, Germany [5]Department of Molecular Toxicology, German Institute of Human Nutrition, Nuthetal, 14558, Germany

[6] Mario Ost and Verena Coleman contributed equally to this work.

*Corresponding author. Tel.: +49 33200 88 2430. E-mail: mario.ost@dife.de (M. Ost).

Received October 19, 2015 • Revision received November 2, 2015 • Accepted November 9, 2015 • Available online 24 November 2015

http://dx.doi.org/10.1016/j.molmet.2015.11.002

[19]. The link between 'browning' and the beneficial pharmacological effects of FGF21 is currently in the focus of metabolic disease research [20–22]. Similarly, a role of myokine FGF21 action in WAT remodeling is speculated [9], suggesting that muscle FGF21 signals to peripheral tissues to enhance substrate utilization/mobilization, although the biological function is debated. On one hand, FGF21 might sequester energy substrates into adipose tissue, thus bypassing the muscle to avoid overload and metabolic stress [23]. Contrarily, muscle FGF21 secretion could be a survival signal to mobilize and supply adequate fuel to the muscle [24]. Notably, oral administration of nicotinamide riboside (vitamin B3) effectively delayed disease progression in Deletor mice, a finding which was linked to even higher levels of circulating FGF21 and protective mitochondrial unfolded protein response (UPR^{mt}) in skeletal muscle [25]. Nevertheless, the ultimate functional relevance of muscle FGF21 as a stress hormone and how it controls systemic, metabolic adaptation has not been delineated yet. Very recently, studying the preprogeroid polymerase gamma mutator (POLG) mouse as a model of mitochondrial disease and premature aging, it was proposed that hepatic FGF21 and high fat diet (HFD) intake cooperatively mediate the rescue of mitochondrial stress [26]. Given the (not only translational) potential of these findings and in order to understand the physiological function of endogenous FGF21, we sought to further explore the specific pathophysiological relevance of skeletal muscle FGF21 in the context of cell-non-autonomous and cell-autonomous muscle mitochondrial stress adaptation and systemic energy metabolism.

The above described models of skeletal muscle autophagy deficiency [9,27] and mitochondrial dysfunction [8,26] show severe muscle disease phenotypes. Thus, we made use of UCP1 transgenic (TG) mice with an ectopic expression of the uncoupling protein 1 (UCP1) in skeletal muscle [28], an established model of metabolic perturbations by muscle-specific decrease in mitochondrial efficiency through increased respiratory uncoupling [29] linked to robust metabolic adaptations [30,31], obesity resistance and increased longevity [32,33]. In addition to the integrated stress response (ISR) induced FGF21 [10], TG mice share a common adaptive metabolic stress response with other models of mitochondrial dysfunction, including muscle proteostasis and amino acid biosynthetic pathways [34]. Curiously, while the idea of a systematic and protective role of endogenous FGF21 is widely accepted in the field, detailed, *in-vivo*, proof-of-principal experiments using genetic ablation of FGF21 are still lacking. Thus, in a cross of TG with *Fgf21*-knockout ($FGF21^{-/-}$) mice [35] we aimed to investigate the functional role of FGF21 as a muscle stress-induced myokine under low and high fat feeding conditions.

2. MATERIAL AND METHODS

2.1. Animals

Experiments were performed in adult male mice that were group-housed and random-caged with *ad libitum* access to food and water at 23 °C and a 12:12 h dark–light cycle. UCP1 transgenic (TG) mice [28] were crossed with *Fgf21*-knockout ($FGF21^{-/-}$) mice [35] to generate four genotypes: wild-type (WT), $FGF21^{-/-}$, TG and TG/$FGF21^{-/-}$ mice. Unless otherwise stated, all data are from male mice at 40 wks of age fed a low-fat (LFD) or a high-fat diet (HFD) [36] for 24 weeks starting at wk 16 of age. Animal experiments were approved by the ethics committee of the Ministry of Agriculture and Environment (State Brandenburg, Germany, permission number GZ V3-2347-16-2013).

2.2. Phenotypical assessments

For representative computed tomography of mice the 3rd generation computed tomography scanner, LaTheta LCT-200 (Hitachi-Aloka, Tokyo, Japan) was used [37]. Body composition was determined by quantitative magnetic resonance (QMR, EchoMRI 2012 Body Composition Analyzer, Houston, USA). Bone mineral density was determined by Dual-energy X-ray absorptiometry (DEXA, Lunar Piximus). Physical locomotor activity was assessed by measurement of spontaneous physical activity using infrared detections (TSE Systems GmbH, Germany). For the oral glucose tolerance test, 2 mg glucose per g body weight was applied 2 h after food withdrawal. Blood glucose levels were measured before, 15, 30, 60 and 120 min after glucose application using a glucose sensor (Bayer, Germany). Insulin levels were measured before, 15 and 30 min after application by an ultra-sensitive ELISA assay (DRG Instruments GmbH, Germany).

2.3. Microarray analysis

Agilent 8 × 60 k whole-genome mouse microarrays (G4852A, Agilent Technologies Inc., Santa Clara, USA) were used. Amplification, labeling, and microarray hybridization of individual sWAT samples of 40 wks old male WT, $FGF21^{-/-}$, TG and TG/$FGF21^{-/-}$ mice ($n = 10$ per group) fed a LFD were performed following the Agilent's procedure for whole-genome microarray technology with a few modifications together with normalization and statistical analysis as described previously [38]. Briefly, One-way ANOVA with FDR-adjustment was used based on all 4 groups ($n = 10$) and $p < 0.05$ was used as threshold for principal component analysis (PCA). This subset of 4983 probes was ranked on fold change of TG over TG/$FGF21^{-/-}$, collapsed into unique genes and only known protein-encoding genes were selected to construct the heat map of the top30 genes (thus excluding Riken cDNA genes and lincRNAs). All microarray data follow minimal information about microarray experiment compliance (MIAME) and have been deposited into the gene expression omnibus (GEO) under accession GSE71749.

2.4. RNA isolation and gene expression analysis

RNA isolation and quantitative real-time PCR was performed as described before [31]. Quadriceps was used for analysis of SM gene expression unless otherwise stated. Multi-tissue gene expression was calculated as dCT using *Hprt* or beta-2 microglobulin (*B2m*) for normalization. *Atf4*: forward primer 5′-GGAATGGCCGGCTATGG-3′, reverse primer 5′-TCCCGGAAAAGGCATCCT-3′; *Gdf15*: forward primer 5′ GAGCTAGGGGTCGCTTC 3′, reverse primer 5′-GGGACCCCAATCTCACCT-3′; *Psat1*: forward primer 5′-AGTGGAGCGCCAGAATAGAA-3′, reverse primer 5′-CTTCGGTTGTGACAGCGTTA-3′; *Slc3a2*: forward primer 5′-CAAAGTGCCAAGAAAAAGAGC-3′, reverse primer 5′-CTGAGCAGGGAGGAACCAC-3′; *Mthfd2*: forward primer 5′-CATGGGGCGTGTGGGAGATAAT-3′, reverse primer 5′-CCGGGCCGTTCGTGAGC-3′; *Fgf21*: forward primer 5′-GCTGCTGGAGGACGGTTACA-3′, reverse primer 5′-CACAGGTCCCCAGGATGTTG-3′; *Atf5*: forward primer 5′-CTACCCCTCCATTCCACTTTCC-3′, reverse 5′-TTCTTGACTGGCTTCTCACTTGTG-3′; *Cd36*: forward primer 5′-CCAAGCTATTGCGACATGAT-3′, reverse primer 5′-ACAGCGTAGATAGACCTGCAAA-3′.

2.5. Analysis of metabolites and circulating factors

FGF21 values were determined by ELISA (Mouse/Rat FGF-21 Quantikine ELISA Kit; R&D Systems) following the manufacturer's instructions. The analysis of triglycerides, free fatty acids and total cholesterol in plasma was performed using an automated analyzer (Cobas Mira S, Hoffmann-La Roche, Basel, Switzerland) with the appropriate commercially available reagent kits (triglycerides,

cholesterol CP, ABX, Montpellier, France; and NEFA; HR, Wako, Neuss, Germany). Metabolite concentrations were determined using a targeted metabolomic approach with the Absolute IDQ®p180 kit (BIOCRATES Life Science AG, Innsbruck, Austria). Sample preparation and measurements were performed as described in the Biocrates user's manual UM-P180- Waters-2. Sample separation and analyte detection were carried out with an Acquity UPLC system connected to a Xevo TQ triple quadrupole mass spectrometer (all from Waters, Eschborn, Germany).

2.6. Enzyme activity assays

Triglyceride concentration in liver was analyzed as described previously [31]. Cytochrome c oxidase (COX) activity in sWAT & BAT and citrate synthase (CS) activity in muscle & BAT [10], together with total muscle glutathione peroxidase (GPx) activity determination was performed as described previously [34].

2.7. Histology

Liver, quadriceps skeletal muscle, sWAT and eWAT were fixed in 4% formaldehyde, embedded in paraffin and cut into 2 μm slices. Hematoxylin-eosin (H&E) staining (Roth, Fluka) was performed to visualize nuclear and cytoplasmic sections within the cell. Freshly dissected femora were collected in ice-cold PBS. Immediately after cleaning bones from surrounding soft tissue, bones were fixed and decalcified in Richard-Allan Scientific™ Cal-Rite™ solution (Thermo Scientific) for 48 h followed by embedding in paraffin. For phenotypic analysis at least three sections of each specimen were made at 6 μm intervals. Sections were stained with H&E (Roth, Fluka).

2.8. Western blotting

Protein was prepared from frozen liver, skeletal muscle (quadriceps) and sWAT. Protein isolation, immunoblotting and detection were performed as previously described [10,39]. Immunoblots were performed using following antibodies: oxidative phosphorylation complexes (OXPHOS, MitoSciences/Abcam, #MS604), PHGDH (Proteintech, #14719-1-AP), UCP1 (Abcam, #ab23841), PPARGC1α + β (Abcam, #ab72230), alpha-Tubulin (αTubulin, Sigma Aldrich, #T6074), phosphor-AMPK^{Thr172} (pAMPK, Cell Signaling, #2531), total-AMPK (tAMPK, Cell Signaling, #2603), CD36/FAT (R&D Systems, #MAB2519), CLPP (Proteintech, #15698-1-AP), MTHFD2 (Santa Cruz Biotechnology, #sc-74985), HSP25 (Enzo life sciences, #ADI-SPA-801), TXN2 (Cell Signaling, #13322).

2.9. FACS analysis

Brown and inguinal fat pads, representing iBAT and sWAT, respectively, were cut in small pieces and incubated with 2 mg/mL collagenase II for 60 min. The cell suspension was filtered through a 100 μm nylon mesh, and the stromal vascular fraction (SVF) was isolated by centrifugation at 1200 rpm for 10 min. The SVF was treated with ACK buffer for 3 min and filtered through a 40 μm nylon mesh. For FACS analysis, erythrocyte-free SVF cells were incubated with a mix of antibodies against different surface markers and sorted using an Aria flow cytometer (BD Biosciences). Briefly, dead cells were removed using propidium iodide staining. Cells negative for CD45/CD31, and positive for SCA1 were considered as APCs [40].

2.10. Statistics

Statistical analyses were performed using Stat Graph Prism (6.0) (GraphPad, San Diego, CA). For microarray bioinformatics, see section above. Data are reported as mean + SEM. After testing for normal distribution (D'Agostino & Pearson omnibus normality test), either One-way ANOVA was used to evaluate differences between genotypes with Bonferroni's multiple comparisons test or Kruskal–Wallis and Dunn's multiple comparison test was used as non-parametric test. Statistical significance was assumed at $p < 0.05$.

3. RESULTS

3.1. Phenotypic characterization of TG/FGF21$^{-/-}$ mice as a model of muscle mitochondrial stress in the absence of endogenous FGF21

We compared male mice of the following four genotypes: wild-type (WT), FGF21$^{-/-}$, TG, and TG/FGF21$^{-/-}$ mice. Phenotype data from mice fed LFD or HFD for 24 weeks (wks) from 16 wks of age confirmed that TG mice with mild muscle mitochondrial stress were smaller and showed reduced bone mass (Figure S1A and B), although they did not show any conspicuous anatomical changes (Figure 1A), compared to control littermates (WT and FGF21$^{-/-}$ mice, Figure S1A). Moreover, TG mice were leaner and resistant to diet-induced obesity compared to control mice (Figure 1B,C + Figure S1C and D). Irrespective of the diet, TG mice showed increased plasma FGF21 levels (Figure 1D) while physical activity levels (Figure 1E) and body temperature (Figure S1E) were not affected. These results are in accordance with the pharmacological effects of FGF21 treatment or with FGF21-overexpression promoting distinct metabolic responses [5,41,42]. Unexpectedly, despite the loss of circulating FGF21 (Figure 1D), the phenotype of TG/FGF21$^{-/-}$ mice was almost identical to TG mice. Further, in contrast to prior expectations [9,26], endogenous FGF21 played only a minor role in regulating body weight gain and fat depot mass under LFD or HFD conditions (Figure 1A–D + Figure S1). Strikingly, we obtained similar results from mice fed LFD or HFD for 16 wks starting from 8 wks of age (Figure S2A–G). Furthermore, absolute energy expenditure was reduced in both TG groups, demonstrating that FGF21 is expendable (Figure S1F). Additionally, energy intake and energy expenditure normalized to body weight (Figure 1F,G + Figure S1G and H) as well as respiratory quotient (Figure 1H) revealed no effect of FGF21 as a myokine.

3.2. Muscle mitochondrial stress-induced WAT browning is fully FGF21-dependent

Next, we investigated adipose tissue as the major target tissues of FGF21 action [43]. Independent of FGF21, white fat depot weights were reduced in TG mice and TG/FGF21$^{-/-}$ mice under LFD and particularly HFD conditions as compared to control littermates at 24 wks and 40 wks of age (Figure S1D + Figure S2G). TG mice on LFD displayed multiple clusters of multilocular adipocytes in subcutaneous WAT (sWAT) depot (Figure 2A) whereas the morphology of epididymal WAT (eWAT) was not affected (Figure S3A). In mice and humans, a link between FGF21 and BAT activity has been shown [22,44]. However, enzyme activity of cytochrome c oxidase (COX) and citrate synthase (CS) measured in interscapular BAT (iBAT), as well as adipogenic progenitor cell population analysis of iBAT stromal vascular fraction using FACS analysis, revealed little differences between the groups (Figure S2B–E), excluding iBAT as a major target of muscle FGF21. In accordance with the morphological appearance of sWAT (Figure 2A), biochemical analysis showed a robust increase of COX activity on LFD in sWAT of TG mice only (Figure 2B) which was largely attenuated on HFD. The molecular extent of sWAT browning was further confirmed by protein induction of PPARGC1α/β, mitochondrial OxPhos complexes and UCP1. These effects were completely absent in TG/FGF21$^{-/-}$mice (Figure 2C). Intriguingly, FGF21-dependent sWAT browning in TG mice was also strongly suppressed by HFD.

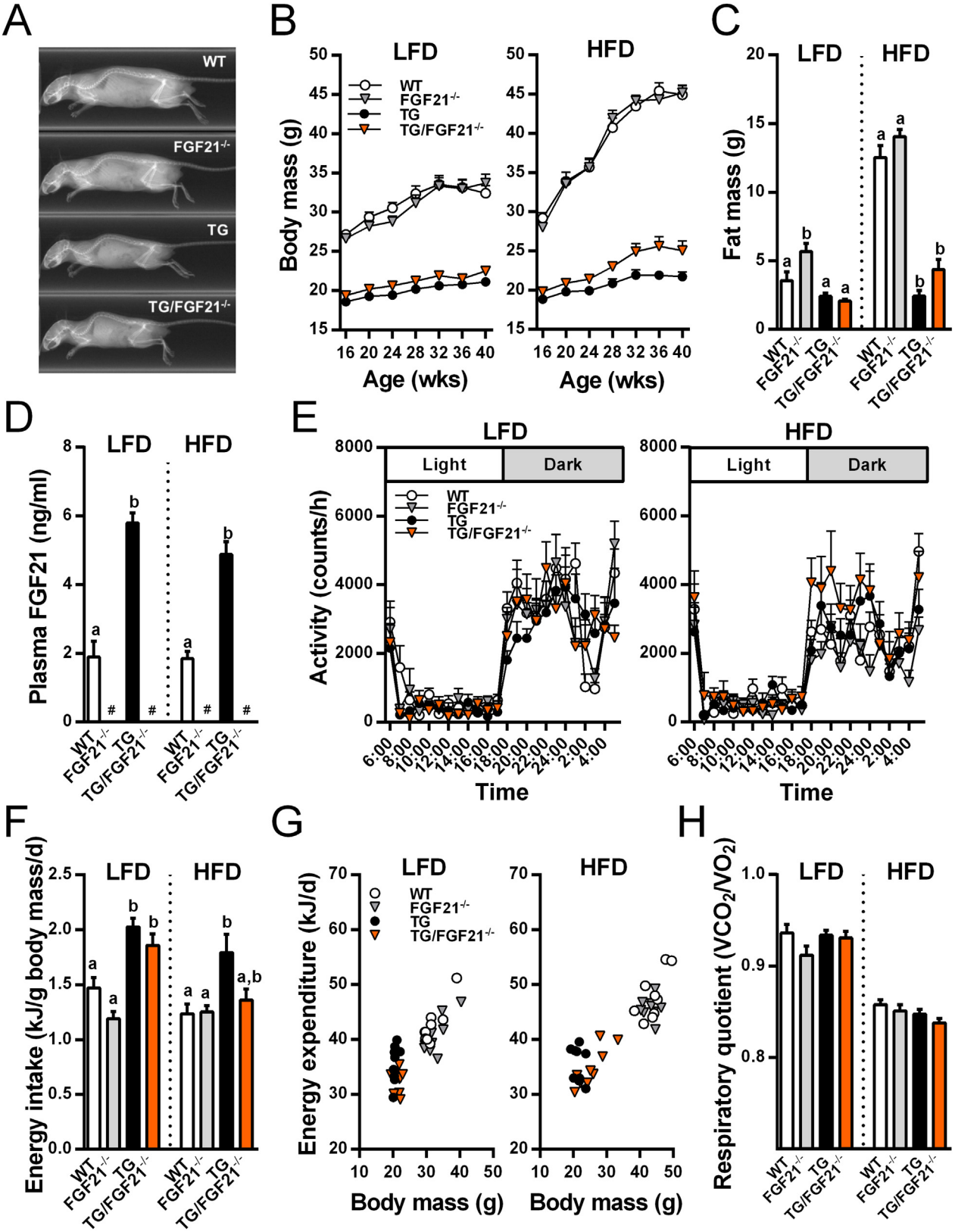

Figure 1: Muscle mitochondrial stress-driven whole body metabolic adaptations do not require FGF21 action. Phenotype data of 40 weeks (wks) old male WT, FGF21$^{-/-}$, TG, and TG/FGF21$^{-/-}$ mice fed low-fat (LFD) or high-fat diet (HFD) for 24 wks. (A) Representative X-ray Computed Tomography (CT)-scan (left panel) of 10 wks old and body length (right panel) of 40 wks old mice (n = 9–10). (B) Body weight development and (C) fat mass determined by quantitative magnetic resonance at wk 40 (n = 9–11). (D) Plasma FGF21 concentration at wk 40 (n = 5–11). (E) Physical activity level, (F) weight specific energy intake, (G) daily energy expenditure (kJ/d) as a function of body mass, and (H) mean 24 h respiratory quotient (VCO_2/VO_2) at wk 36 (n = 9–11). Except of (G) all data represent mean + SEM; means with different letters are significantly different; #, not detectable.

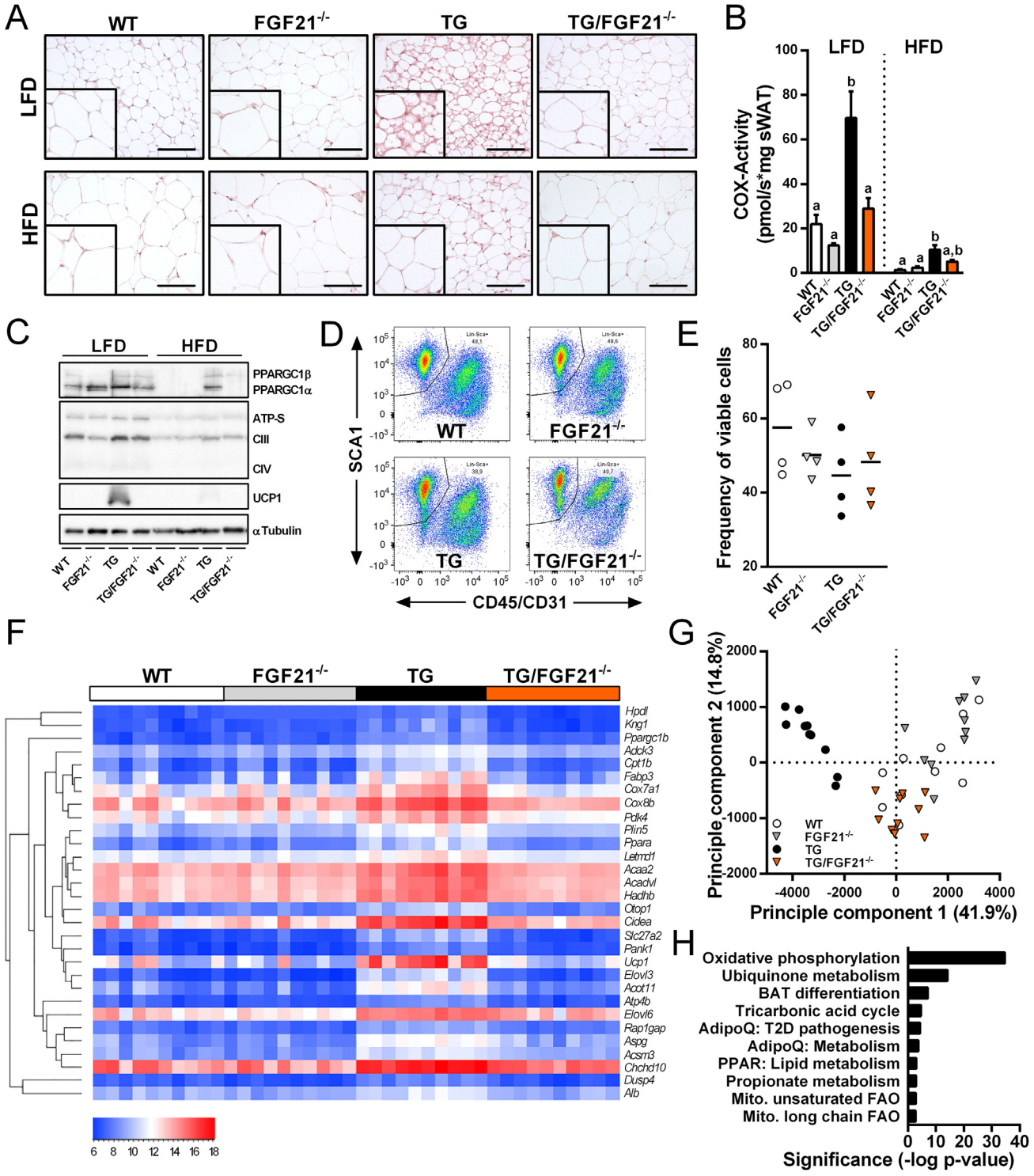

Figure 2: Muscle mitochondrial stress-induced WAT browning is fully FGF21-dependent. (A–C) Subcutaneous WAT (sWAT) of 40 weeks (wks) old male WT, FGF21$^{-/-}$, TG, and TG/FGF21$^{-/-}$ mice fed low-fat (LFD) or high-fat diet (HFD) for 24 wks (A) sWAT morphology (H&E); bars represent 50 μm. (B) Cytochrome c oxidase (COX) activity per mg sWAT tissue (n = 9–11). (C) Representative immunoblots of UCP1, PPARGC1α/β and mitochondrial OxPhos complexes (CIII, Complex 3 core protein 2; CIV, Complex 4 subunit I; ATP-S, ATP-Synthase alpha subunit); α-Tubulin was used as loading control. (D) FACS analysis and (E) quantification of frequency of SCA1^{+}/Lin^{-}(CD45/CD31) progenitor cells from sWAT stromal vascular fraction (SVF) of young male mice at 8 wks of age (n = 4). (F–H) Transcriptomic profiling of FGF21-dependent metabolic remodeling in sWAT from 40 wk old males mice fed LFD (n = 10 per group). (F) Heat map of gene expression levels of the top 30 most significant regulated genes using whole genome microarray analysis (ANOVA FDR $p < 0.0005$ followed by FC TG over TG/FGF21$^{-/-}$). (G) Principal component analysis (PCA) showing the distinct profile of TG mice compared to the all other groups using One-way ANOVA-FDR ($p < 0.05$; 4983 probes). (H) Pathway enrichment analysis using MetaCore (FC > 1.15, FDR-adjusted $p < 0.05$); FAO, fatty acid beta-oxidation; T2D, Type 2 diabetes. All data represent mean + SEM; means with different letters are significantly different.

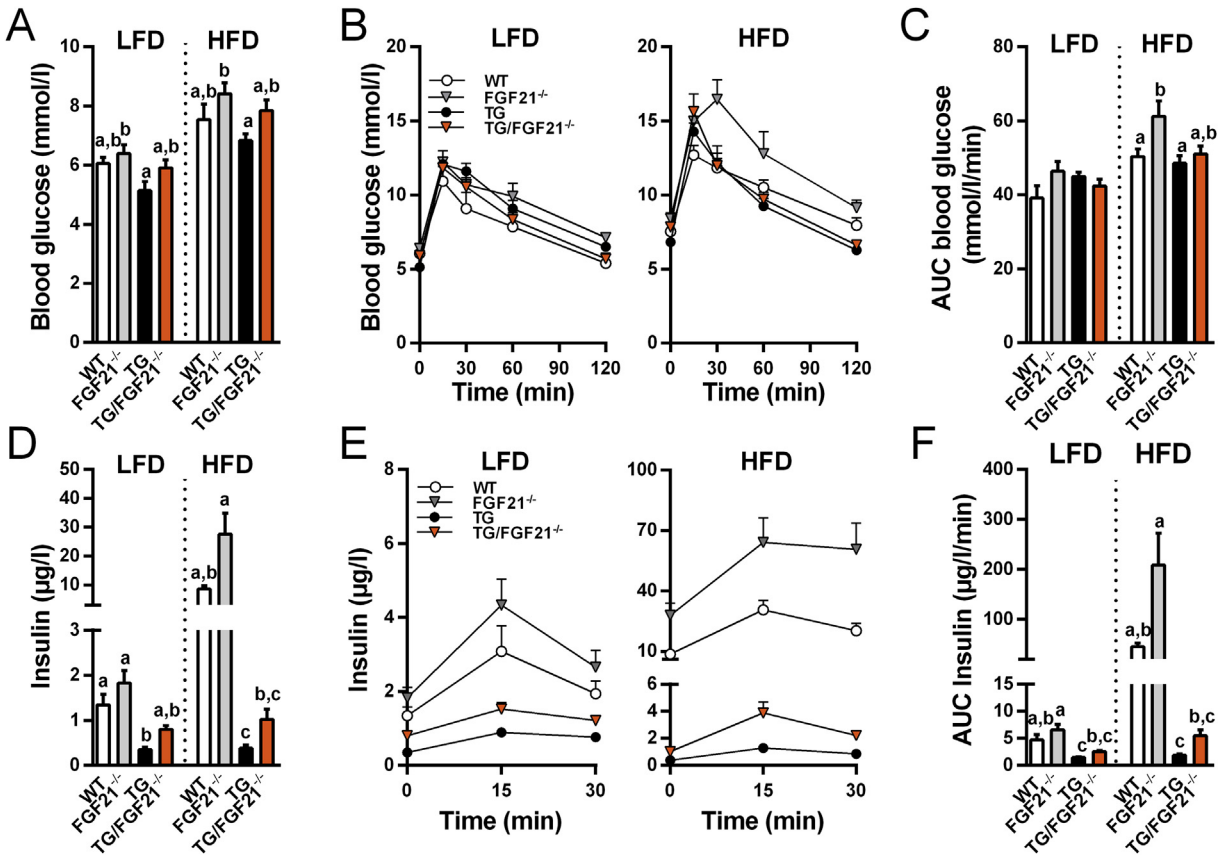

Figure 3: FGF21 action is dispensable for muscle mitochondrial stress-improved glycemic control. Phenotype data of 40 weeks (wks) old male WT, FGF21$^{-/-}$, TG, and TG/FGF21$^{-/-}$ mice fed low-fat (LFD) or high-fat diet (HFD) for 24 wks. (A) Basal blood glucose in postabsorptive state and (B) during an oral glucose tolerance test (oGTT) together with (C) the corresponding total area under curve of blood glucose during oGTT at wk 38 (n = 9–11). (D) Basal plasma insulin levels in postabsorptive state and (E) during the oGTT together with (F) the corresponding total area under curve of insulin during oGTT. All data represent mean + SEM; means with different letters are significantly different.

To examine whether the FGF21-induced browning under LFD conditions was due to changes in precursor cell populations, we performed FACS analysis in sWAT stromal vascular fraction of young male mice. Quantification of adipogenic SCA1^{+}/Lin^{-}(CD45/CD31) progenitor cells [40] showed no differences between the groups (Figure 2D,E). To identify key mechanisms of myokine-induced adipose tissue remodeling, we next performed whole genome gene expression analysis in sWAT of male mice on LFD. Gene clustering and principal component analysis (PCA) showed that gene expression profile (Figure 2F,G) of TG sWAT was distinct from the other three groups. A heat map of the 30 most upregulated genes in sWAT of TG mice includes BAT-markers *Ucp1*, *Acot11*, *Cidea*, *Cox7a1*, *Cpt1a*, *Elovl3*, *Fabp3*, *Ppargc1b* and *Ppara* (Figure 2F, full gene names are listed in Table S1). In addition, pathway enrichment analysis using MetaCore revealed a robust and unique browning transcriptome pattern in sWAT of TG mice, including oxidative phosphorylation, mitochondrial ubiquinone metabolism signaling and BAT-differentiation (Figure 2H, for details see also Table S2). Strikingly, this gene expression profile was fully absent in TG/FGF21$^{-/-}$ mice although both TG genotypes displayed a similar fat depot mass.

3.3. FGF21 action is dispensable for muscle mitochondrial stress-improved glycemic control

Apart from the muscle mitochondrial stress-induced anti-obesogenic effects, the improved whole body insulin sensitivity also was recently related to FGF21 induction and WAT metabolic activation [9,11]. In line with that, the induction of recruitable brown adipocytes, also called beige cells, has been linked not only to obesity resistance but also to improved glucose homeostasis [45]. As mentioned above, we here performed two long-term diet intervention studies (Figure 1 and Figure S2). Surprisingly, despite the absence of FGF21 action and sWAT browning, we observed that glucose tolerance did not differ between TG and TG/FGF21$^{-/-}$ mice in both studies (Figure 3A–C + Figure S2H and I). Intriguingly, comparing all groups, FGF21$^{-/-}$ mice were most susceptible to HFD-induced impairment of glycemic control. Additionally, plasma insulin levels during oral glucose tolerance test were strongly reduced in both TG and TG/FGF21$^{-/-}$ mice (Figure 3D–F + Figure S2J and K), in particular under HFD conditions. Remarkably, this effect was again independent of WAT browning and diet intervention. Thus, improved glycemic control and insulin sensitivity induced by muscle mitochondrial stress occurred independent of FGF21, suggesting that FGF21 as myokine is of little significance for the systemic adaptation of glucose metabolism.

3.4. Differential role of muscle FGF21 on plasma and hepatic lipid homeostasis

Browning of WAT has been associated with improved metabolic health, including diminished hepatic lipid content and attenuated dyslipidemia [46]. Thus, we further evaluated parameters of plasma and hepatic lipid homeostasis. Plasma triglycerides and cholesterol were

significantly lower in TG mice than in the other three genotypes, independent of diet and sWAT browning, whereas plasma free fatty acids were not affected (Figure 4A–C). The induction of FGF21 as stress-induced myokine was recently related to improved hepatic metabolic profile and whole-body metabolic homeostasis [9]. In contrast, we here clearly demonstrate a negligible role of muscle mitochondrial stress-induced FGF21 in hepatic lipid homeostasis. Histological analyses showed that although HFD induced hepatic steatosis in WT and FGF21$^{-/-}$ mice, very little intracellular hepatic lipid accumulation was observed in TG and TG/FGF21$^{-/-}$ mice on HFD (Figure 4D) consistent with reduced hepatic triglyceride content (Figure 4E). HFD did not lead to an induction of hepatic *Fgf21* gene

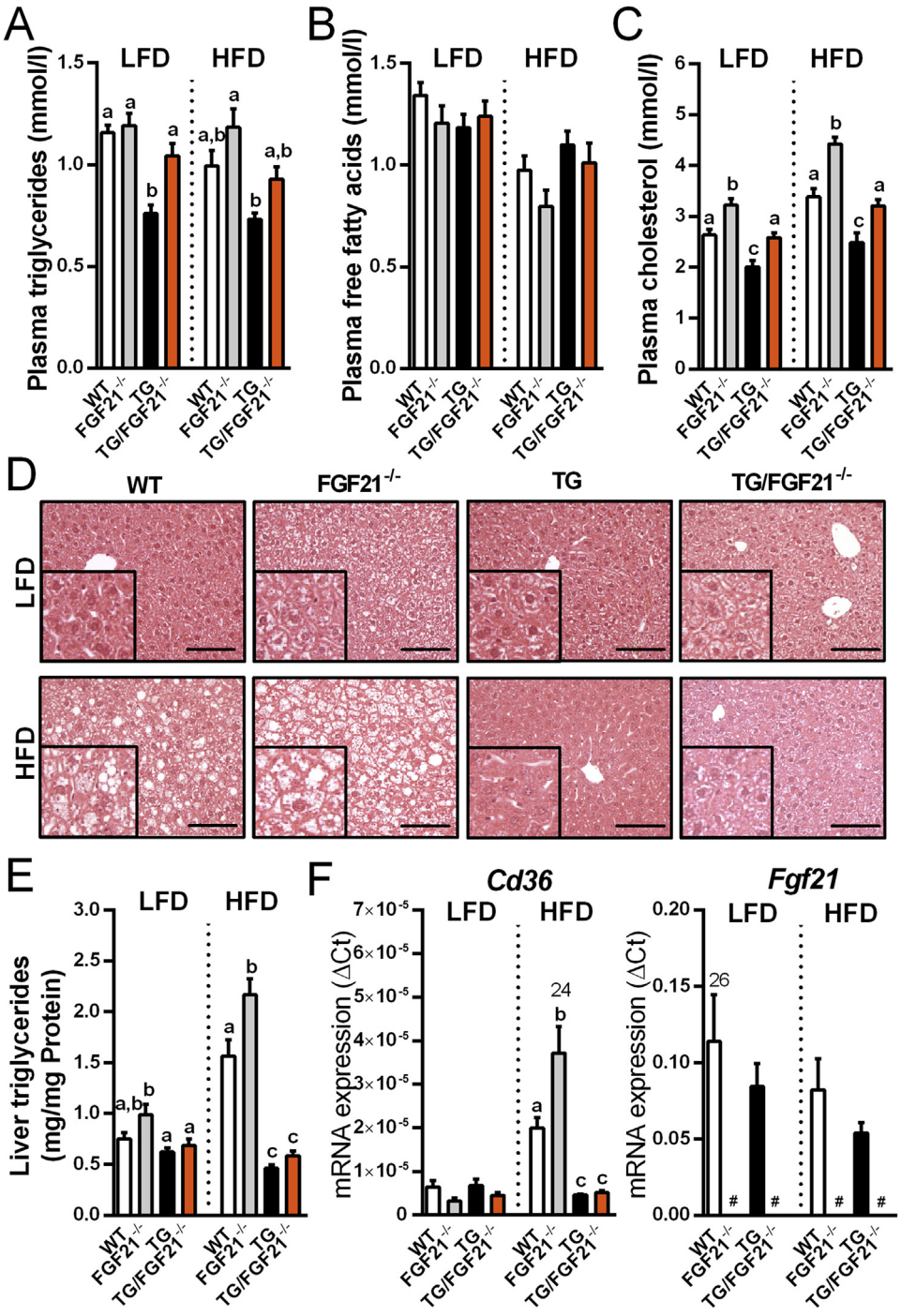

Figure 4: Differential role of muscle FGF21 on plasma and hepatic lipid homeostasis. Plasma and liver analyses of 40 weeks (wks) old male WT, FGF21$^{-/-}$, TG, and TG/FGF21$^{-/-}$ mice fed low-fat (LFD) or high-fat diet (HFD) for 24 wks. (A) Plasma triglycerides, (B) free fatty acids, and (C) cholesterol levels (mmol/l) (n = 9). (D) Liver morphology (H&E); bars represent 50 μm. (E) Liver triglyceride content (mg) per mg protein (n = 9–11 per group). (F) qPCR of hepatic *Cd36* (fatty acid translocase FAT/CD36) and *Fgf21* gene expression (n = 8); qPCR cycle time values are displayed for the group with highest expression level. All data represent mean + SEM; means with different letters are significantly different.

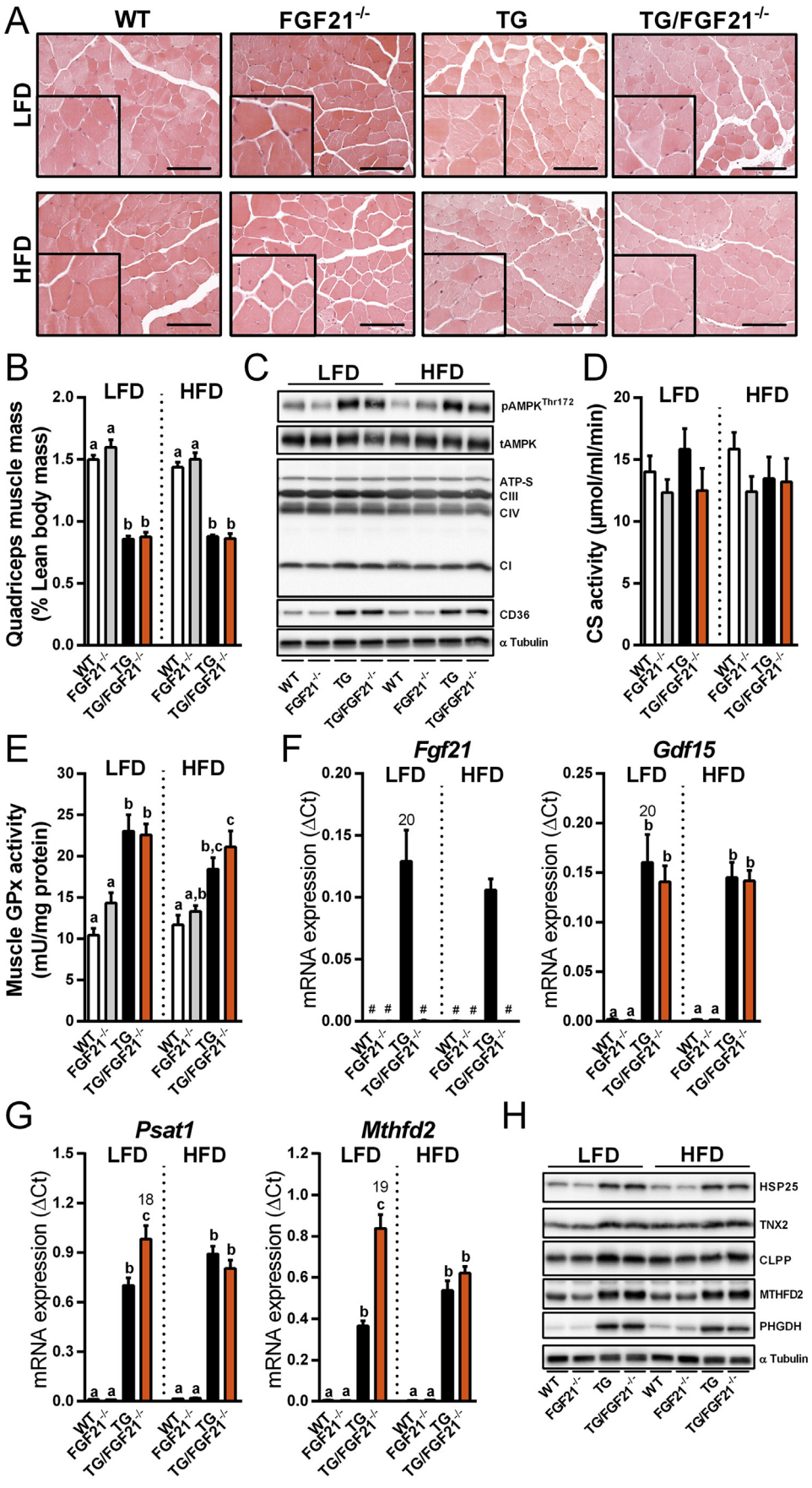

expression whereas it highly increased hepatic gene expression of the fatty acid translocase *Cd36* in control mice, which was completely abolished in both TG and TG/FGF21$^{-/-}$ mice (Figure 4F). Thus, despite the significant effects on sWAT remodeling, muscle secreted FGF21 had only minor effects on plasma and hepatic lipid homeostasis.

3.5. Metabolic rescue of mitochondrial stress in muscle operates independent of FGF21 action

The precise pathophysiological relevance of mitochondrial stress-induced FGF21 especially for skeletal muscle itself is still poorly understood. Recent *in-vitro* studies proposed muscle FGF21 as a compensatory cell-autonomous stress response to improve mitochondrial function [47]. However, independent of FGF21 action and diet, skeletal muscle morphology was preserved (Figure 5A), despite a greatly reduced muscle mass in both TG and TG/FGF21$^{-/-}$ mice (Figure 5B). Strikingly, the induction of phospho-AMPK^{Thr172} and the fatty acid translocase CD36 in muscle of TG mice were not affected by the loss of FGF21 action (Figure 5C). Furthermore, in line with a preserved mitochondrial OxPhos complex protein expression (Figure 5C), muscle mitochondrial content evaluated by citrate synthase (CS) activity was also not affected by FGF21 ablation (Figure 5D). Further, muscle glutathione peroxidase (GPx) activity as marker of cellular oxidative stress response remained increased in TG/FGF21$^{-/-}$ mice (Figure 5E). In addition, the robust gene expression induction of the myokines *Fgf21* and *Gdf15*, as shown previously in TG mice [10,34], could be confirmed, the latter similar in both TG and TG/FGF21$^{-/-}$ (Figure 5F). Recently, we described a detailed profile of muscle metabolic remodeling [34] adding to the already established mitochondrial stress-related pseudo-starvation response [8]. In agreement with these studies, key markers related the serine, one-carbon, glycine (SOG) pathway (*Psat1*, *Mthfd2*) were induced in skeletal muscle of TG mice (Figure 5G). This metabolic profile was still preserved in the absence of FGF21, excluding FGF21 as control element of the pseudo-starvation response. Remarkably, immunoblots of UPR^{mt} marker proteins HSP25, TNX2 and ATP-dependent CLPP as well as selected SOG pathway proteins PHGDH and MTHFD2 in muscle showed no differences between TG and TG/FGF21$^{-/-}$ mice (Figure 5H), demonstrating that muscle metabolic remodeling and mitohormetic response does not require FGF21 action.

4. DISCUSSION

FGF21 currently receives general interest as one of the most promising clinical anti-diabetic drug candidate [4], but, paradoxically, circulating endogenous FGF21 is elevated during obesity [48,49], type 2 diabetes [50], and coronary artery disease [51]. In contrast, its induction and secretion from skeletal muscle in response to mitochondrial perturbations and ISR activation [8–11] raised the idea of an adaptive mitochondrial stress-related pseudo-starvation response via endogenous FGF21. However, previous studies so far only speculated on the beneficial metabolic role of FGF21, whereas detailed long-term proof-of-principle experiments using genetic ablation of FGF21 were lacking. Here, we conclusively tested this hypothesis using the established UCP1 transgenic mouse [28,31,33], a model of muscle mitochondrial perturbations and a recently published common metabolic remodeling profile [34], together with a comprehensive array of FGF21-ablated mouse models and dietary challenges. Surprisingly, we found new evidence supporting a dispensable role of FGF21 for muscle cell-autonomous as well as systemic metabolic adaptations.

One effect that is clearly dependent on endogenous FGF21 action is the browning of sWAT induced by muscle mitochondrial stress in a cell-non-autonomous manner. The first to suggest an induction of browning by endogenous FGF21 was the group of Bruce Spiegelman who showed that FGF21-deficient mice displayed diminished cold induced browning of WAT. During cold exposure, FGF21 expression was found to be increased in different adipose depots suggesting an autocrine/paracrine manner of action [19]. Here we enlarge this concept to endocrine acting muscle FGF21. Surprisingly, since the study of Fisher et al. [19] our study is the only one to investigate browning in FGF21$^{-/-}$ mice. Several studies have shown that FGF21 treatment or overexpression is associated with a browning of WAT [52–54] but without demonstrating that the observed browning was actually dependent on FGF21. Notably, browning of WAT has been associated with improved metabolic profiles making this an interesting target to combat obesity associated disorders [46]. On the other hand, recent studies found that WAT browning can also contribute to body weight loss and cachexia in cancer patients [55,56]. Moreover, WAT browning can also be induced by circulating metabolites from muscle in response to exercise [57]. Noteworthy, *Fndc5*/irisin, the only other myokine reported to induce WAT browning [58], is not induced by respiratory uncoupling in muscle [10,39]. Overall, although the browning of WAT has been well established in different rodent models and also in humans, its precise physiological function and relevance remain hotly debated [59]. Here we show that FGF21-dependent browning is attenuated by HFD. This is not attributable to obesity, i.e. WAT expansion, because it is also observed in TG mice, which did not increase WAT mass on HFD. The attenuation of WAT browning by HFD thus seems to be related to dietary fat intake itself and suggests that it might play a role in lipid/fatty acid metabolism and homeostasis. In line with this, previous studies on Deletor and POLG mice showed that mitochondrial dysfunction is associated with lipid metabolic alterations, which can be compensated by a ketogenic or high-lipid diet [8,26,60]. Additionally, the muscle mitochondrial-stress related reduction of plasma triglycerides and cholesterol was abolished in the absence of FGF21, similarly under low and high fat feeding conditions. Browning of sWAT in general was largely attenuated by HFD questioning its role in these metabolic improvements. Further studies are warranted to examine the interaction of dietary fat and the mitochondrial stress-induced metabolic fine-tuning including WAT remodeling.

In contrast to previous studies on muscle autophagy-deficient mice [9], our study on TG/FGF21$^{-/-}$ mice clearly shows that mitochondrial

Figure 5: Metabolic rescue of mitochondrial stress in muscle operates independent of FGF21. Muscle analyses of 40 weeks (wks) old male WT, FGF21$^{-/-}$, TG, and TG/FGF21$^{-/-}$ mice fed low-fat (LFD) or high-fat diet (HFD) for 24 wks. (A) Muscle (tibialis anterior) morphology; bars represent 50 μm. (B) Quadriceps muscle mass (n = 9–11). (C) Representative immunoblots of pAMPK^{Thr172}/tAMPK, mitochondrial OxPhos complexes (CI, Complex 1 subunit NDUFB8; CIII, Complex 3 core protein 2; CIV, Complex 4 subunit I; ATP-S, ATP-Synthase alpha subunit) and fatty acid translocase FAT/CD36 (CD36). (D) Citrate synthase (CS) activity in m. gastrocnemius (n = 5). (E) Total glutathione peroxidase (GPx) activity in m. quadriceps (n = 9–11). (F–G) qPCR of myokines (*Fgf21*; *Gdf15*, growth differentiation factor 15) and key markers of SOG pathway (*Psat1*, phosphoserine aminotransferase 1; *Mthfd2*, methylentetrahydrofolate dehydrogenase 2) (n = 8); qPCR cycle time values are displayed for the group with highest expression level. (H) Representative immunoblots of UPR^{mt} marker proteins HSP25 (heat shock protein 25), TNX2 (thioredoxin-2), CLPP (Clp protease) and key SOG pathway proteins (MTHFD2; PHGDH, phosphoglycerate dehydrogenase). qPCR and immunoblots were performed in m. quadriceps; α-Tubulin was used as loading control. All data represent mean + SEM; means with different letters are significantly different. #, not detectable.

stress-promoted obesity resistance and glycemic control occurs independently of endogenous FGF21, suggesting that it is of little significance for a systemic adaptive response. Noteworthy, autophagy plays a crucial role in the regulation of cellular processes to maintain skeletal muscle integrity and function [27,61]. Thus, the metabolic response through disruption of autophagy studied by Kim et al. [9] may not arise from mitochondrial-specific stress but rather from a general impaired cellular homeostasis which requires FGF21 action. However, the metabolic profile of muscle autophagy-deficient mice under HFD conditions was still improved when crossed with FGF21$^{-/-}$ mice, whereas standard/LFD conditions and the issues of FGF21-dependent WAT/BAT activation as well as cell-autonomous muscle ISR were not investigated at all [9]. Moreover, to our knowledge, there are presently no data available on Deletor and POLG mice with genetic ablation of FGF21. Nevertheless, although the different muscle-specific metabolic stress mouse models are based on distinct genetic manipulations [8–10], they all show a common adaptive response including the induction of muscle ER stress-mediated FGF21 and amino acid biosynthetic pathways [34]. In the present study, we show that the common mitochondrial stress-related pseudo-starvation response [8,34], including key markers related to the serine, one-carbon, glycine (SOG) pathway, was still highly induced in TG/FGF21$^{-/-}$ mice. This indicates that the muscle cell-autonomous metabolic remodeling occurs independently of endogenous FGF21, which needs to be confirmed in other described mitochondrial stress mouse models.

If not FGF21, what might be the key mediators for muscle mitochondrial stress response? It is generally accepted that multiple organ crosstalk involves both cell-autonomous and cell-non-autonomous mechanisms [62]. Importantly, AMPK as a key regulator of cellular energy homeostasis and cell-autonomous stress adaption [39,63,64] was still activated in the absence of FGF21. Moreover, we here confirm that muscle mitochondrial stress promotes the expression of *Gdf15*, encoding a cytokine of the TGF-β superfamily (also known as MIC-1/NAG-1). This is in line with a recent transcriptomic study on mitochondrial myopathy patients [65]. Notably, we here show that the induction of *Gdf15* was not affected by the loss of FGF21 action. It was previously shown that overexpression of *Gdf15* in mice prevents diet-induced obesity and increases lifespan by activating adipose tissue as well as systemic energy metabolism [66,67]. Conversely, circulating levels of GDF15 are also highly elevated in patients with muscle atrophy [68] and in cancer patients with severe anorexia and weight loss [69] and chronic inflammation [70]. Hence, future studies are required to delineate the protective or detrimental role of GDF15 as mitochondrial stress-induced cytokine. Moreover, further efforts are warranted to identify additional critical cell-non-autonomous mediators of muscle mitochondrial stress adaptation, independent of endogenous FGF21.

5. CONCLUSION

The endocrine acting pleiotropic protein FGF21 was proposed as key metabolic mediator of the mitochondrial stress adaptation. Notably, we here confirmed that WAT is a major target of circulating myokine FGF21. However, in contrast to prior expectations [9–11,26], the present study on TG/FGF21$^{-/-}$ mice as a model of muscle mitochondrial stress in the absence of endogenous FGF21 clearly shows that the adaptive metabolic stress response operates independently of both WAT browning and FGF21 action. Thus, our data are pivotal for the progressively emerging concept of cell-non-autonomous and cell-autonomous muscle mitochondrial pseudo-starvation response. Taken together, these findings challenge FGF21 as a powerful therapeutic target during muscle mitochondrial disease and future studies are required to identify other, yet unknown adaptive processes apart from FGF21.

AUTHOR CONTRIBUTIONS

MO and SK designed and conducted the study; VC, AV and MO performed animal experiments, collected and analyzed most of the data except from: EvS and IvdS performed microarray analysis and bioinformatics; SKei performed COX- and CS-activity assay in BAT; SR performed liver sample analysis; AG performed FACS analysis in adipose tissue, TA performed bone histology, MO, VC and SK wrote the paper, which was proof-read and corrected by all authors, who all contributed to data evaluation.

ACKNOWLEDGMENTS

We would like to thank Antje Sylvester, Carolin Borchert, Susann Richter and Stefanie Deubel for technical assistance and Dr. Nobuyuki Itoh for providing FGF21$^{-/-}$ mice [35]. This research received funding from the Leibniz Society (SAW-2013-FBN-3).

CONFLICT OF INTERESTS

The authors declare no conflict of interest.

APPENDIX A. SUPPLEMENTARY DATA

Supplementary data related to this article can be found at http://dx.doi.org/10.1016/j.molmet.2015.11.002.

REFERENCES

[1] Kharitonenkov, A., Larsen, P., 2011. FGF21 reloaded: challenges of a rapidly growing field. Trends in Endocrinology & Metabolism 22:81–86.
[2] Inagaki, T., Dutchak, P., Zhao, G., Ding, X., Gautron, L., Parameswara, V., et al., 2007. Endocrine regulation of the fasting response by PPARalpha-mediated induction of fibroblast growth factor 21. Cell Metabolism 5:415–425.
[3] Owen, B.M., Ding, X., Morgan, D.A., Coate, K.C., Bookout, A.L., Rahmouni, K., et al., 2014. FGF21 acts centrally to induce sympathetic nerve activity, energy expenditure, and weight loss. Cell Metabolism 20:670–677.
[4] Kharitonenkov, A., Adams, A.C., 2014. Inventing new medicines: the FGF21 story. Molecular Metabolism 3:221–229.
[5] Badman, M.K., Pissios, P., Kennedy, A.R., Koukos, G., Flier, J.S., Maratos-Flier, E., 2007. Hepatic fibroblast growth factor 21 is regulated by PPARalpha and is a key mediator of hepatic lipid metabolism in ketotic states. Cell Metabolism 5:426–437.
[6] Muise, E.S., Azzolina, B., Kuo, D.W., El-Sherbeini, M., Tan, Y., Yuan, X., et al., 2008. Adipose fibroblast growth factor 21 is up-regulated by peroxisome proliferator-activated receptor gamma and altered metabolic states. Molecular Pharmacology 74:403–412.
[7] Izumiya, Y., Bina, H.A., Ouchi, N., Akasaki, Y., Kharitonenkov, A., Walsh, K., 2008. FGF21 is an Akt-regulated myokine. FEBS Letters 582:3805–3810.
[8] Tyynismaa, H., Carroll, C.J., Raimundo, N., Ahola-Erkkila, S., Wenz, T., Ruhanen, H., et al., 2010. Mitochondrial myopathy induces a starvation-like response. Human Molecular Genetics 19:3948–3958.
[9] Kim, K.H., Jeong, Y.T., Oh, H., Kim, S.H., Cho, J.M., Kim, Y.N., et al., 2013. Autophagy deficiency leads to protection from obesity and insulin resistance by inducing Fgf21 as a mitokine. Nature Medicine 19:83–92.
[10] Keipert, S., Ost, M., Johann, K., Imber, F., Jastroch, M., van Schothorst, E.M., et al., 2014. Skeletal muscle mitochondrial uncoupling drives endocrine cross-

talk through the induction of FGF21 as a myokine. American Journal of Physiology Endocrinology and Metabolism 306:E469–482.
[11] Tsai, S., Sitzmann, J.M., Dastidar, S.G., Rodriguez, A.A., Vu, S.L., McDonald, C.E., et al., 2015. Muscle-specific 4E-BP1 signaling activation improves metabolic parameters during aging and obesity. Journal of Clinical Investigation 125:2952–2964.
[12] Hojman, P., Pedersen, M., Nielsen, A.R., Krogh-Madsen, R., Yfanti, C., Akerstrom, T., et al., 2009. Fibroblast growth factor-21 is induced in human skeletal muscles by hyperinsulinemia. Diabetes 58:2797–2801.
[13] Hansen, J.S., Clemmesen, J.O., Secher, N.H., Hoene, M., Drescher, A., Weigert, C., et al., 2015. Glucagon-to-insulin ratio is pivotal for splanchnic regulation of FGF-21 in humans. Molecular Metabolism 4:551–560.
[14] Crooks, D.R., Natarajan, T.G., Jeong, S.Y., Chen, C., Park, S.Y., Huang, H., et al., 2014. Elevated FGF21 secretion, PGC-1alpha and ketogenic enzyme expression are hallmarks of iron-sulfur cluster depletion in human skeletal muscle. Human Molecular Genetics 23:24–39.
[15] Suomalainen, A., Elo, J.M., Pietilainen, K.H., Hakonen, A.H., Sevastianova, K., Korpela, M., et al., 2011. FGF-21 as a biomarker for muscle-manifesting mitochondrial respiratory chain deficiencies: a diagnostic study. Lancet Neurology 10:806–818.
[16] Nunnari, J., Suomalainen, A., 2012. Mitochondria: in sickness and in health. Cell 148:1145–1159.
[17] Ogawa, Y., Kurosu, H., Yamamoto, M., Nandi, A., Rosenblatt, K.P., Goetz, R., et al., 2007. BetaKlotho is required for metabolic activity of fibroblast growth factor 21. Proceedings of the National Academy of Sciences U S A 104:7432–7437.
[18] Lin, Z., Tian, H., Lam, K.S., Lin, S., Hoo, R.C., Konishi, M., et al., 2013. Adiponectin mediates the metabolic effects of FGF21 on glucose homeostasis and insulin sensitivity in mice. Cell Metabolism 17:779–789.
[19] Fisher, F.M., Kleiner, S., Douris, N., Fox, E.C., Mepani, R.J., Verdeguer, F., et al., 2012. FGF21 regulates PGC-1alpha and browning of white adipose tissues in adaptive thermogenesis. Genes & Development 26:271–281.
[20] Veniant, M.M., Sivits, G., Helmering, J., Komorowski, R., Lee, J., Fan, W., et al., 2015. Pharmacologic effects of FGF21 are independent of the "Browning" of white adipose tissue. Cell Metabolism 21:731–738.
[21] Samms, R.J., Smith, D.P., Cheng, C.C., Antonellis, P.P., Perfield 2nd, J.W., Kharitonenkov, A., et al., 2015. Discrete aspects of FGF21 in vivo pharmacology do not require UCP1. Cell Reports 11:991–999.
[22] Keipert, S., Kutschke, M., Lamp, D., Brachthauser, L., Neff, F., Meyer, C.W., et al., 2015. Genetic disruption of uncoupling protein 1 in mice renders brown adipose tissue a significant source of FGF21 secretion. Molecular Metabolism 4:537–542.
[23] Fisher, F.M., Maratos-Flier, E., 2013. Stress heats up the adipocyte. Nature Medicine 19:17–18.
[24] Luo, Y., McKeehan, W.L., 2013. Stressed liver and muscle call on adipocytes with FGF21. Frontiers in Endocrinology 4:194.
[25] Khan, N.A., Auranen, M., Paetau, I., Pirinen, E., Euro, L., Forsstrom, S., et al., 2014. Effective treatment of mitochondrial myopathy by nicotinamide riboside, a vitamin B3. EMBO Molecular Medicine 6:721–731.
[26] Wall, C.E., Whyte, J., Suh, J.M., Fan, W., Collins, B., Liddle, C., et al., 2015. High-fat diet and FGF21 cooperatively promote aerobic thermogenesis in mtDNA mutator mice. Proceedings of the National Academy of Sciences U S A 112:8714–8719.
[27] Masiero, E., Agatea, L., Mammucari, C., Blaauw, B., Loro, E., Komatsu, M., et al., 2009. Autophagy is required to maintain muscle mass. Cell Metabolism 10:507–515.
[28] Klaus, S., Rudolph, B., Dohrmann, C., Wehr, R., 2005. Expression of uncoupling protein 1 in skeletal muscle decreases muscle energy efficiency and affects thermoregulation and substrate oxidation. Physiological Genomics 21:193–200.
[29] Keipert, S., Klaus, S., Heldmaier, G., Jastroch, M., 2010. UCP1 ectopically expressed in murine muscle displays native function and mitigates mitochondrial superoxide production. Biochimica Biophysica Acta 1797:324–330.
[30] Neschen, S., Katterle, Y., Richter, J., Augustin, R., Scherneck, S., Mirhashemi, F., et al., 2008. Uncoupling protein 1 expression in murine skeletal muscle increases AMPK activation, glucose turnover, and insulin sensitivity in vivo. Physiological Genomics 33:333–340.
[31] Keipert, S., Ost, M., Chadt, A., Voigt, A., Ayala, V., Portero-Otin, M., et al., 2013. Skeletal muscle uncoupling-induced longevity in mice is linked to increased substrate metabolism and induction of the endogenous antioxidant defense system. American Journal of Physiology-Endocrinology and Metabolism 304:E495–E506.
[32] Keipert, S., Voigt, A., Klaus, S., 2011. Dietary effects on body composition, glucose metabolism, and longevity are modulated by skeletal muscle mitochondrial uncoupling in mice. Aging Cell 10:122–136.
[33] Gates, A.C., Bernal-Mizrachi, C., Chinault, S.L., Feng, C., Schneider, J.G., Coleman, T., et al., 2007. Respiratory uncoupling in skeletal muscle delays death and diminishes age-related disease. Cell Metabolism 6:497–505.
[34] Ost, M., Keipert, S., van Schothorst, E.M., Donner, V., van der Stelt, I., Kipp, A.P., et al., 2015. Muscle mitohormesis promotes cellular survival via serine/glycine pathway flux. FASEB Journal: Official Publication of the Federation of American Societies for Experimental Biology 29:1314–1328.
[35] Hotta, Y., Nakamura, H., Konishi, M., Murata, Y., Takagi, H., Matsumura, S., et al., 2009. Fibroblast growth factor 21 regulates lipolysis in white adipose tissue but is not required for ketogenesis and triglyceride clearance in liver. Endocrinology 150:4625–4633.
[36] Hoevenaars, F.P., van Schothorst, E.M., Horakova, O., Voigt, A., Rossmeisl, M., Pico, C., et al., 2012. BIOCLAIMS standard diet (BIOsd): a reference diet for nutritional physiology. Genes Nutrition 7:399–404.
[37] Lubura, M., Hesse, D., Neumann, N., Scherneck, S., Wiedmer, P., Schurmann, A., 2012. Non-invasive quantification of white and brown adipose tissues and liver fat content by computed tomography in mice. PLoS One 7:e37026.
[38] Hoek-van den Hil, E.F., van Schothorst, E.M., van der Stelt, I., Swarts, H.J., Venema, D., Sailer, M., et al., 2014. Quercetin decreases high-fat diet induced body weight gain and accumulation of hepatic and circulating lipids in mice. Genes Nutrition 9:418.
[39] Ost, M., Werner, F., Dokas, J., Klaus, S., Voigt, A., 2014. Activation of AMPKalpha2 is not crucial for mitochondrial uncoupling-induced metabolic effects but required to maintain skeletal muscle integrity. Plos One 9:e94689.
[40] Schulz, T.J., Huang, T.L., Tran, T.T., Zhang, H., Townsend, K.L., Shadrach, J.L., et al., 2011. Identification of inducible brown adipocyte progenitors residing in skeletal muscle and white fat. Proceedings of the National Academy of Sciences U S A 108:143–148.
[41] Inagaki, T., Lin, V.Y., Goetz, R., Mohammadi, M., Mangelsdorf, D.J., Kliewer, S.A., 2008. Inhibition of growth hormone signaling by the fasting-induced hormone FGF21. Cell Metabolism 8:77–83.
[42] Coskun, T., Bina, H.A., Schneider, M.A., Dunbar, J.D., Hu, C.C., Chen, Y., et al., 2008. Fibroblast growth factor 21 corrects obesity in mice. Endocrinology 149:6018–6027.
[43] Adams, A.C., Yang, C., Coskun, T., Cheng, C.C., Gimeno, R.E., Luo, Y., et al., 2012. The breadth of FGF21's metabolic actions are governed by FGFR1 in adipose tissue. Molecular Metabolism 2:31–37.
[44] Lee, P., Linderman, J.D., Smith, S., Brychta, R.J., Wang, J., Idelson, C., et al., 2014. Irisin and FGF21 are cold-induced endocrine activators of brown fat function in humans. Cell Metabolism 19:302–309.
[45] Harms, M., Seale, P., 2013. Brown and beige fat: development, function and therapeutic potential. Nature Medicine 19:1252–1263.
[46] Bartelt, A., Heeren, J., 2014. Adipose tissue browning and metabolic health. Nature Reviews Endocrinology 10:24–36.

[47] Ji, K., Zheng, J., Lv, J., Xu, J., Ji, X., Luo, Y.B., et al., 2015. Skeletal muscle increases FGF21 expression in mitochondrial disorders to compensate for energy metabolic insufficiency by activating the mTOR-YY1-PGC1alpha pathway. Free Radical Biology & Medicine 84:161—170.

[48] Zhang, X., Yeung, D.C., Karpisek, M., Stejskal, D., Zhou, Z.G., Liu, F., et al., 2008. Serum FGF21 levels are increased in obesity and are independently associated with the metabolic syndrome in humans. Diabetes 57:1246—1253.

[49] Berti, L., Irmler, M., Zdichavsky, M., Meile, T., Bohm, A., Stefan, N., et al., 2015. Fibroblast growth factor 21 is elevated in metabolically unhealthy obesity and affects lipid deposition, adipogenesis, and adipokine secretion of human abdominal subcutaneous adipocytes. Molecular Metabolism 4:519—527.

[50] Mashili, F.L., Austin, R.L., Deshmukh, A.S., Fritz, T., Caidahl, K., Bergdahl, K., et al., 2011. Direct effects of FGF21 on glucose uptake in human skeletal muscle: implications for type 2 diabetes and obesity. Diabetes/Metabolism Research and Reviews 27:286—297.

[51] Shen, Y., Ma, X., Zhou, J., Pan, X., Hao, Y., Zhou, M., et al., 2013. Additive relationship between serum fibroblast growth factor 21 level and coronary artery disease. Cardiovascular Diabetology 12:124.

[52] Emanuelli, B., Vienberg, S.G., Smyth, G., Cheng, C., Stanford, K.I., Arumugam, M., et al., 2014. Interplay between FGF21 and insulin action in the liver regulates metabolism. Journal of Clinical Investigation 124:515—527.

[53] Camporez, J.P., Jornayvaz, F.R., Petersen, M.C., Pesta, D., Guigni, B.A., Serr, J., et al., 2013. Cellular mechanisms by which FGF21 improves insulin sensitivity in male mice. Endocrinology 154:3099—3109.

[54] Lee, P., Werner, C.D., Kebebew, E., Celi, F.S., 2014. Functional thermogenic beige adipogenesis is inducible in human neck fat. International Journal of Obesity 38:170—176.

[55] Kir, S., White, J.P., Kleiner, S., Kazak, L., Cohen, P., Baracos, V.E., et al., 2014. Tumour-derived PTH-related protein triggers adipose tissue browning and cancer cachexia. Nature 513:100—104.

[56] Petruzzelli, M., Schweiger, M., Schreiber, R., Campos-Olivas, R., Tsoli, M., Allen, J., et al., 2014. A switch from white to brown fat increases energy expenditure in cancer-associated cachexia. Cell Metabolism 20:433—447.

[57] Roberts, L.D., Bostrom, P., O'Sullivan, J.F., Schinzel, R.T., Lewis, G.D., Dejam, A., et al., 2014. beta-Aminoisobutyric acid induces browning of white fat and hepatic beta-oxidation and is inversely correlated with cardiometabolic risk factors. Cell Metabolism 19:96—108.

[58] Bostrom, P., Wu, J., Jedrychowski, M.P., Korde, A., Ye, L., Lo, J.C., et al., 2012. A PGC1-alpha-dependent myokine that drives brown-fat-like development of white fat and thermogenesis. Nature 481:463—468.

[59] Nedergaard, J., Cannon, B., 2014. The browning of white adipose tissue: some burning issues. Cell Metabolism 20:396—407.

[60] Ahola-Erkkila, S., Carroll, C.J., Peltola-Mjosund, K., Tulkki, V., Mattila, I., Seppanen-Laakso, T., et al., 2010. Ketogenic diet slows down mitochondrial myopathy progression in mice. Human Molecular Genetics 19:1974—1984.

[61] Masiero, E., Sandri, M., 2010. Autophagy inhibition induces atrophy and myopathy in adult skeletal muscles. Autophagy 6:307—309.

[62] Schinzel, R., Dillin, A., 2015. Endocrine aspects of organelle stress-cell nonautonomous signaling of mitochondria and the ER. Current Opinion in Cell Biology 33:102—110.

[63] Bujak, A.L., Crane, J.D., Lally, J.S., Ford, R.J., Kang, S.J., Rebalka, I.A., et al., 2015. AMPK activation of muscle autophagy prevents fasting-induced hypoglycemia and myopathy during aging. Cell Metabolism 21:883—890.

[64] Jager, S., Handschin, C., St-Pierre, J., Spiegelman, B.M., 2007. AMP-activated protein kinase (AMPK) action in skeletal muscle via direct phosphorylation of PGC-1alpha. Proceedings of the National Academy of Sciences U S A 104:12017—12022.

[65] Kalko, S.G., Paco, S., Jou, C., Rodriguez, M.A., Meznaric, M., Rogac, M., et al., 2014. Transcriptomic profiling of TK2 deficient human skeletal muscle suggests a role for the p53 signalling pathway and identifies growth and differentiation factor-15 as a potential novel biomarker for mitochondrial myopathies. BMC Genomics 15:91.

[66] Chrysovergis, K., Wang, X., Kosak, J., Lee, S.H., Kim, J.S., Foley, J.F., et al., 2014. NAG-1/GDF-15 prevents obesity by increasing thermogenesis, lipolysis and oxidative metabolism. International Journal of Obesity 38:1555—1564.

[67] Wang, X., Chrysovergis, K., Kosak, J., Kissling, G., Streicker, M., Moser, G., et al., 2014. hNAG-1 increases lifespan by regulating energy metabolism and insulin/IGF-1/mTOR signaling. Aging (Albany NY) 6:690—704.

[68] Bloch, S.A., Lee, J.Y., Syburra, T., Rosendahl, U., Griffiths, M.J., Kemp, P.R., et al., 2015. Increased expression of GDF-15 may mediate ICU-acquired weakness by down-regulating muscle microRNAs. Thorax 70:219—228.

[69] Johnen, H., Lin, S., Kuffner, T., Brown, D.A., Tsai, V.W., Bauskin, A.R., et al., 2007. Tumor-induced anorexia and weight loss are mediated by the TGF-beta superfamily cytokine MIC-1. Nature Medicine 13:1333—1340.

[70] Breit, S.N., Johnen, H., Cook, A.D., Tsai, V.W., Mohammad, M.G., Kuffner, T., et al., 2011. The TGF-beta superfamily cytokine, MIC-1/GDF15: a pleotrophic cytokine with roles in inflammation, cancer and metabolism. Growth Factors 29:187—195.

